

Compression-rate dependence of the phase transition from hexagonal ice to ice II and/or ice III

Marion Bauer,¹ Michael S. Elsaesser,² Katrin Winkel,¹ Erwin Mayer,¹ and Thomas Loerting^{2,*}

¹*Institute of General, Inorganic, and Theoretical Chemistry, University of Innsbruck, Innrain 52a, A-6020 Innsbruck, Austria*

²*Institute of Physical Chemistry, University of Innsbruck, Innrain 52a, A-6020 Innsbruck, Austria*

(Received 2 June 2008; published 27 June 2008)

We study the density-driven phase transition from hexagonal ice in the temperature range of 170–230 K up to pressures of 0.65 GPa using a piston-cylinder apparatus. Pure ice II, pure ice III, or mixtures of ice II and ice III are identified as products when the compression-rate is varied from 0.001–4 GPa/min. At low compression-rates and at high temperatures, formation of ice II is observed, which is in accordance with the phase diagram. However, at low temperatures and at higher compression rates, formation of metastable ice III is observed, which extends the known temperature range for possible formation of ice III. Metastable ice III rather than stable ice II crystals are produced by simple variation of the compression rate, which is an uncommon concept of producing metastable phases. We discuss some implications for our understanding of the interior of icy satellites such as Ganymede.

DOI: 10.1103/PhysRevB.77.220105

PACS number(s): 62.50.-p, 64.60.My, 81.30.Hd, 96.30.-t

Polymorphism, i.e., the ability of a solid material to exist in more than one crystal structure, is an important scholarly concept, which is of practical relevance, e.g., in pharmaceutical industry. Water has a very rich phase diagram. Currently, 15 polymorphs of ice are experimentally verified (including the metastable ones).¹ All ice on earth, including the ice buried in glaciers, is hexagonal ice (ice Ih). In the atmosphere also some cubic ice (ice Ic) may be present.² In the earth's interior the high-pressure polymorph ice VII is speculated to form in subduction zones and may be responsible for some seismic events.^{3,4} Some high-pressure polymorphs of ice are expected to occur naturally in the interior of satellites of the planets from Jupiter outward, namely, in the Galilean satellites: Europa, Ganymede, and Callisto, six Saturn and five Uranus moons, and the Pluto/Charon system.⁵⁻⁸ These icy satellites can be covered by up to 900 km of ice shell, which has in some cases even differentiated by the slow unmixing of rock and ice in the history of the moon. The ice crust is probably separated into a sequence of concentric shells of high-pressure polymorphs depending on the distance to surface and temperature. In the case of Europa and Callisto it is debated whether a salty subsurface ocean or a rheologically weak polymorph of ice are present today.⁷⁻⁹ In Fig. 1 the stable polymorphs of ice up to 2.5 GPa are shown. The shaded area shows an approximate temperature/pressure path when moving from the surface of the icy satellites toward their centers.¹⁰ One would expect the ice crust of icy satellites to be composed of the sequence ice Ih-ice II-ice V-ice VI from this plot. Sohl *et al.*¹¹ on the other hand assume the sequence ice Ih-ice III-ice V-ice VI, i.e., the occurrence of the metastable high-pressure polymorphs of ice III within the stability field of ice II. Here we show by variation of the compression rate that stable pure ice II, metastable pure ice III, as well as mixtures of the two can form under p and T conditions relevant to the interior of icy satellites. Here we present a systematic investigation of the influence of compression rate on high-pressure phase transitions.

Ice II and Ice III were the first high-pressure polymorphs discovered.^{12,13} The phase boundary between ice II and ice III and the triple point ice Ih-ice II-ice III at 238 K and 0.29 GPa were discovered a few years later.¹⁴ Ice III, once formed, does not convert back to ice II and survives in the

stability field of ice II. In fact, the activation barrier for the transformation from ice III to the stable ice II phase is so high that no measurable conversion takes place.¹⁵ When ice III is prepared on its own field of stability (e.g., at 250 K and 0.35 GPa) and is cooled slowly under isobaric conditions through the stability field of ice II, it remains ice III down to ~ 170 K (Ref. 15) and converts gradually to proton-ordered ice III (called ice IX) below 170 K (Ref. 15). That is, metastable ice III does not convert to ice II in the stability field of ice II but rather to ice IX, which is also metastable with respect to ice II (Ref. 16). The pressurization from ice Ih to the stability field of ice II was studied previously by a number of researchers.¹⁷⁻³⁴ All studies agree that always ice II forms from ice Ih in the temperature range of 170–230 K. However, at temperatures above 230 K, both ice III and ice II were observed,¹⁴ and at temperatures from 150–170 K ice IX (Refs. 23, 26, 29, and 32) or ice II (Ref. 28) can form. Our study concerning the compression-rate dependence now reveals that metastable ice III can also form upon pressurizing ice Ih in the temperature range of 170–230 K. That is, the domain of metastable existence of ice III is extended.

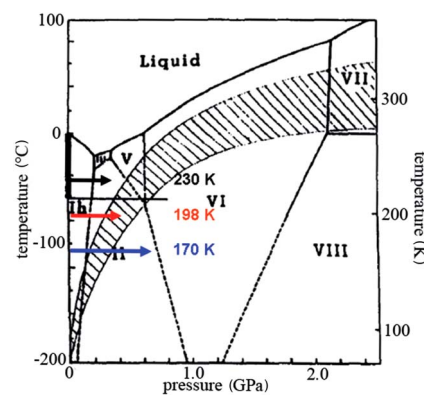


FIG. 1. (Color online) Water's phase diagram of stable phases. The shaded area indicates the approximate pressure and temperature conditions in the interior of the icy satellites of outer planets. The arrows indicate the paths taken for the uniaxial compression experiments of hexagonal ice. The figure was adapted from Leliwa-Kopystynski (Ref. 10).

Kirby and co-workers^{30,31} also studied the rheological properties of ice II and ice III and concluded, in accordance with the data presented by Echelmeyer and Kamb,³⁵ that there is a huge contrast in strength (as defined by viscosity) between ice II and ice III (Refs. 24, 25, 31, 36, and 37). Ice II is a “strong ice,” being even more viscous by four orders of magnitude compared to ice Ih. On the contrary ice III is a “very weak” ice, which flows $\sim 10^3$ times faster than ice II and is also much weaker than ice Ih. At very low grain sizes and low stresses ice II even shows a change in flow mechanism from “dislocation creep” to “diffusion creep” and “superplasticity,” which has important implications for the thermal evolution and internal dynamics of the icy satellites.^{38,39}

Hexagonal ice is produced by pipetting 500 μl of deionized water into the bore (8 mm in diameter) of the cylinder, which is cooled at approximately 77 K by immersion in liquid nitrogen and lined with 300 mg of indium for low-temperature lubrication. Next, the system is brought to a constant temperature of 170, 198, or 230 K by removing liquid nitrogen and by pumping liquid nitrogen through cooling loops and counterheating using resistive heaters. The system is then compressed (at constant temperature) at approximately 0.30–0.65 GPa using varying compression-rates ranging from 1 to 4000 MPa/min. Under these p - T conditions ice II is the thermodynamically stable phase according to water’s phase diagram. Temperature is routinely measured using a Pt-100 sensor countersunk in the steel cylinder, which is sitting at a distance of about 10 mm to the sample. For two cross-check measurements we have additionally mounted a K -type thermocouple directly within the ice sample. At compression-rates of 80 and 160 MPa/min the difference between the Pt-100 sensor and the K -type thermocouple never exceeds 3 K, i.e., the sample itself does not experience significant frictional heating during compression. Using the same setup we have previously shown that even at compression-rates of 6000 MPa/min the amount of frictional heating produced does not suffice to induce crystallization of amorphous samples kept at 125 K, which would take place for sample temperatures exceeding approximately 145 K (instead of crystallization we have observed amorphous-amorphous transitions).^{40,41} The friction in our setup is in fact so low that we refrain from correcting from “nominal pressure” to “real pressure,” e.g., for a transition taking place at 1.00 GPa the difference between the nominal and real pressures is less than 0.01 GPa. In order to quench the sample and recover it, the cylinder is again immersed in liquid nitrogen prior to decompression to ambient pressure. The sample is then analyzed by powder x-ray diffraction in Θ - Θ geometry at approximately 80 K using $\text{Cu-}K\alpha$ radiation.

In Fig. 2 we show piston displacement curves along with the powder x-ray diffractograms of the recovered samples. In Fig. 2(a) we compare compression experiments at 198 K at the compression rates of 10 and 1000 MPa/min. In these experiments the temperature as read out by the Pt-100 sensor does not vary by more than ± 0.2 K. In other experiments we had observed temperature oscillations by up to ± 1 K. In both experiments shown in Fig. 2(a) there is a sharp density increase as indicated by a step in piston displacement of ~ 1.2 mm. This step indicates a phase transition to a denser

phase. For both experiments the overall densification is very similar thus suggesting that in both cases a phase of about the same density has formed. The onset for the step in density can be found at 0.252 GPa at 10 MPa/min and at 0.267 GPa at 1000 MPa/min. Both of these pressures are indicative of overpressurization—the ice Ih to ice II phase boundary intersects at approximately 0.16 GPa at 198 K. The difference between 0.252 and 0.267 GPa may either be due to sluggish kinetics or due to the formation of a distinct phase. Analysis of the powder x-ray diffractograms of the quench-recovered samples in Fig. 2(b) clearly shows that the latter is the case—two clearly distinct powder x-ray patterns are observed. At the rate of 10 MPa/min the thermodynamically stable phase ice II is observed, whereas at a rate of 1000 MPa/min metastable ice III is observed. The expected peak positions for ice II and ice III are indicated by tiny ticks below and above the diffractograms, respectively. We emphasize that powder x-ray diffraction does not allow distinguishing between proton-ordered ice IX and proton-disordered ice III, which both share a common lattice of oxygen atoms. It is, however, known that ice III protons only order at $T < 170$ K (Ref. 15) and so we rule out formation of ice IX in the temperature range of 170–230 K. Whereas it is probably not possible to produce proton-ordered ice at high temperatures where one would expect proton-disordered ice, it was shown on the example of the ice VII/VIII transition that it is possible to retain proton-disordered ice at low temperatures where one would expect proton-ordered ice.^{42,43} A quantitative analysis using the program “POWDER CELL”⁴⁴ indicates that 100% pure ice II has formed at 10 MPa/min and almost pure ice III with impurities of ice II of less than 10% has formed at 1000 MPa/min. In Fig. 3 we show how the fraction of ice III develops as the compression rate is increased. On increasing the compression rate from 10 to 30 MPa/min, the fraction of ice III increases from 0% to 85%, whereas the fraction of ice II drops from 100% to 15%. As the compression-rate is increased further the remaining fraction of ice II in the ice II/ice III mixture continues to drop and finally reaches 0% at a compression-rate of 4000 MPa/min.

This finding suggests that two parallel modes of nucleation and crystal growth are operating upon pressurizing ice Ih: the first mode nucleates and grows ice II, and the second mode nucleates and grows ice III. While the first mode shows an earlier onset of growth (0.252 vs 0.267 GPa) the second mode shows a faster growth of crystals. This finding is consistent with the data by Durham *et al.*²⁵ who show that the ice I-ice III transition is “nucleation limited,” whereas the ice I-ice II transition is “growth limited.” So, for low compression-rates there is ample time for growth and pure ice II forms, since it nucleates first. On the other hand for high compression-rates there is not enough time for growth of ice II, and pure ice III forms. At intermediate compression-rates there is competition between the two modes and mixtures of ice II and ice III result.

In Figs. 2(c) and 2(d) we show the effect of temperature at a constant compression-rate of 100 MPa/min. At 198 K a mixture of 85% ice III and 15% ice II forms. Upon decreasing the temperature to 170 K pure ice III forms, whereas upon increasing the temperature to 230 K pure ice II forms.

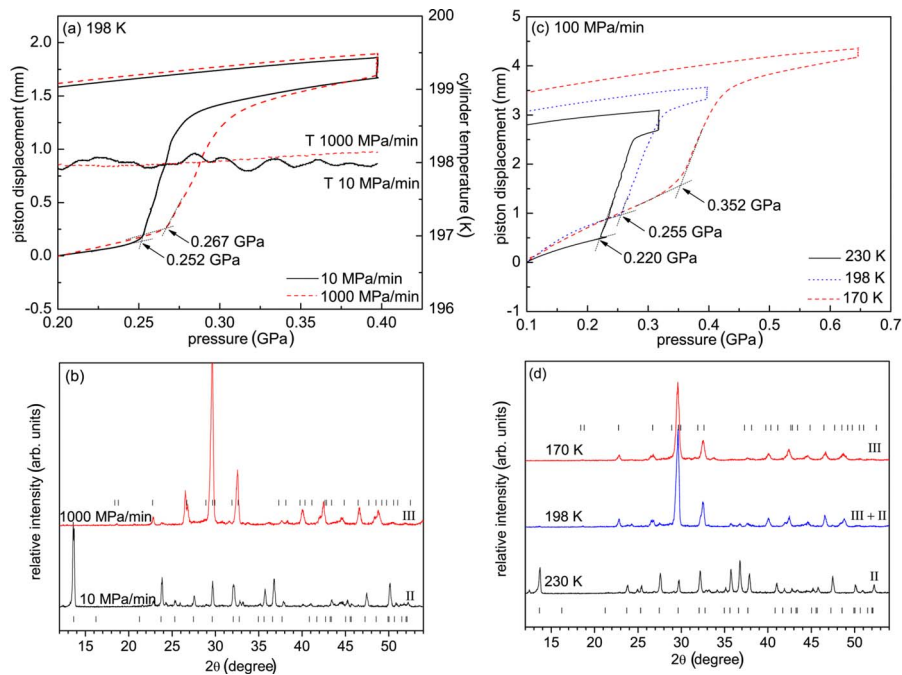


FIG. 2. (Color online) (a) Piston displacement vs nominal pressure curves showing the densification step to ice II at a rate of 10 MPa/min (black solid line) and to ice III at a rate of 1000 MPa/min (red dashed line). The onset of the phase transition is indicated by black dotted tangents. In addition the temperature as read out by the Pt-100 sensor mounted in the steel cylinder 10 mm from the sample is shown (right axis). (b) Powder x-ray diffractograms of the samples shown in (a) after quenching to 77 K and decompression to 1 bar as measured in θ - θ geometry at ~ 80 K using Cu- $K\alpha$ radiation. Ticks close to the powder x-ray diffractograms indicate the expected peak position from the structures of ice II (Refs. 18 and 20) and ice III (Ref. 21). (c) Piston displacement vs nominal pressure curves showing the densification step to ice III at 170 K (red dashed line) to a 85:15 mixture of ice III and ice II at 198 K (blue dotted line) and to ice II at 230 K (black solid line), all at a compression rate of 100 MPa/min. The onset of the phase transition is indicated by black dotted tangents. (d) Powder x-ray diffractograms of the samples shown in (c) after quenching to 77 K and decompression to 1 bar as measured in θ - θ geometry at ~ 80 K using Cu- $K\alpha$ radiation. Ticks close to the powder x-ray diffractograms indicate the expected peak position from the structures of ice II (Refs. 18 and 20) and ice III (Ref. 21).

That is, the thermodynamically stable crystal preferentially grows at higher temperatures, whereas the metastable crystal preferentially grows at lower temperatures. At 150 K ice IX was in fact reported to grow directly from ice Ih (Ref. 26). The increasing amount of ice II with increasing temperature can be rationalized in terms of increasing growth rates. On

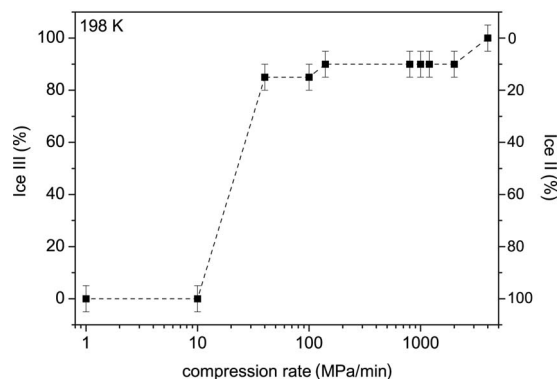


FIG. 3. The effect of variation of compression rate on the fraction of ice III in the ice II/ice III mixture produced by compressing hexagonal ice isothermally at 198 K. The error bars indicate the reliability of the POWDER CELL (Ref. 44) fit of ice II and ice III patterns to the observed powder x-ray diffractograms.

the other hand, at low temperatures, growth of ice II slows down and the fraction of ice III increases. The lower the temperature the easier it is to generate a metastable crystal. Of course, the amount of overpressurization required to transform ice Ih to ice II and/or ice III decreases as the temperature is increased: at 170 K the onset is found at 0.352 GPa, whereas it is found at 230 K at 0.220 GPa.

We finally discuss the implications of our results for the understanding of the interior structure of icy satellites. If the buildup of pressure at low temperatures in the course of the formation of the satellite took place at a time scale of millions of years, then we expect formation and presence of stable ice II according to our results. If on the other hand impacting bodies were responsible for fast pressure buildup and temperature increase resulting in partial melting during the genesis of the icy satellites, then nucleation and growth of ice III is expected. Ice III may either grow from ice Ih crystals as a result of the high compression rate or it may grow upon cooling from the pressurized melt, whereas there is no path for growth of ice II under “impact” conditions. Ice III, once formed, cannot transform to ice II directly—if one wants to make ice II from ice III one has either to melt ice III first or to produce ice Ih by decompression first. Unfortunately, the densities for ice II and ice III are identical to within $\sim 1\%$ [see Fig. 2(a)],¹⁶ and so it is hardly possible to

infer from moments of inertia measurements whether the ice crusts contains ice II or ice III at depths >100 km (where the weight of the ice is sufficient to induce a density-driven phase transition). However, except for the density, ice II or ice III show very distinct properties. Ice II is a proton-ordered phase, whereas ice III is mainly proton-disordered.^{16,45} Transport properties such as heat conductivity or solid-state viscosity and plasticity differ by many orders of magnitude.^{15,25,35,37,46} E.g., ice III is less viscous than ice Ih, whereas ice II is more viscous than ice Ih.

In conclusion, we have shown that two competing mechanisms are operative for the density-driven phase transition of hexagonal ice Ih. One mechanism causes the formation of thermodynamically stable ice II, whereas the other causes the formation of metastable ice III within the ice II stability field. In view of our results ice III formation at 170–230 K is a possibility that has to be taken into account. So far, ice III formation has only been considered within or slightly below the stability field of ice III at $T > 230$ K, whereas ice II formation has been considered at temperatures $T < 240$ K below the stability field of ice III. We have also shown that variation of the compression rate can suppress one mechanism completely in the sense that solely the stable crystal forms at low compression-rates and that solely a metastable

crystal forms at high compression rates. The formation of ice III is not due to frictional heating to temperatures $T > 230$ K where ice III is stable in the phase diagram but rather due to nucleation and crystal growth of metastable ice III within the stability domain of ice II. This offers the exciting perspective of growing metastable crystals also for other substances, e.g., minerals. It is possible that unknown polymorphs may be discovered in the future using the technique of compression-rate variation. We have furthermore shown that it becomes easier to form the metastable crystal (ice III) as the temperature is lowered, e.g., to 170 K. Of course, as the temperature is lowered too far ($T < 145$ K), the transformation will not take place at all for kinetic reasons.^{29,32} While our results do not allow deciding with certainty whether ice II, ice III, or mixtures of the two persist in the interior of icy satellites, our results may provide some clues for the history of the icy satellites once the ice polymorphs in the interior of icy satellites are known with certainty.

We are thankful to David C. Rubie for the helpful discussion and to the Austrian Science Fund (Schrödinger Rückkehr Grant No. R37-N11 and START Grant No. Y391) for the financial support.

*thomas.loerting@uibk.ac.at

- ¹C. G. Salzmann *et al.*, *Science* **311**, 1758 (2006).
- ²B. J. Murray, D. A. Knopf, and A. K. Bertram, *Nature* (London) **434**, 202 (2005).
- ³C. R. Bina and A. Navrotsky, *Nature* (London) **408**, 844 (2000).
- ⁴J.-F. Lin, E. Schwegler, and C.-S. Yoo, *Geophys. Monogr.* **168**, 159 (2006).
- ⁵G. J. Consolmagno and J. S. Lewis, *Icarus* **34**, 280 (1978).
- ⁶G. J. Consolmagno, *J. Phys. Chem.* **87**, 4204 (1983).
- ⁷A. P. Showman and R. Malhotra, *Science* **286**, 77 (1999).
- ⁸F. Sohl *et al.*, *Icarus* **157**, 104 (2002).
- ⁹J. Ruiz, *Nature* (London) **412**, 409 (2001).
- ¹⁰J. Leliwa-Kopystynski, *Adv. Space Res.* **15**, 69 (1995).
- ¹¹F. Sohl *et al.*, *Icarus* **157**, 104 (2002).
- ¹²G. Tammann, *Z. Anorg. Chem.* **63**, 285 (1909).
- ¹³G. Tammann, *Z. Phys. Chem.* **72**, 609 (1910).
- ¹⁴P. W. Bridgman, *Proc. Am. Acad. Arts Sci.* **47**, 439 (1912).
- ¹⁵W. B. Durham *et al.*, *J. Phys. Colloq.* **C1**, C1-221 (1987).
- ¹⁶V. F. Petrenko and R. W. Whitworth, *Physics of Ice* (Oxford University Press, Oxford, 1999).
- ¹⁷J. E. Bertie, L. D. Calvert, and E. Whalley, *J. Chem. Phys.* **38**, 840 (1963).
- ¹⁸B. Kamb, *Acta Crystallogr.* **17**, 1437 (1964).
- ¹⁹E. D. Finch *et al.*, *J. Chem. Phys.* **49**, 4361 (1968).
- ²⁰B. Kamb *et al.*, *J. Chem. Phys.* **55**, 1934 (1971).
- ²¹B. Kamb and A. Prakash, *Acta Crystallogr., Sect. B: Struct. Crystallogr. Cryst. Chem.* **24**, 1317 (1968).
- ²²O. Mishima and S. Endo, *J. Chem. Phys.* **73**, 2454 (1980).
- ²³B. Minceva—Sukarova, W. F. Sherman, and G. R. Wilkinson, *J. Phys. C* **17**, 5833 (1984).
- ²⁴S. H. Kirby, W. B. Durham, and H. C. Heard, *NATO ASI Ser., Ser. C* **156**, 89 (1985).
- ²⁵W. B. Durham *et al.*, *J. Geophys. Res.* **93**, 10191 (1988).
- ²⁶A. K. Garg, *Phys. Status Solidi A* **110**, 467 (1988).
- ²⁷Y. P. Handa, D. D. Klug, and E. Whalley, *Can. J. Chem.* **66**, 919 (1988).
- ²⁸S. H. Kirby, W. B. Durham, and L. A. Stern, in *Physics and Chemistry of Ice*, edited by N. Maeno and T. Hondoh (Hokkaido University Press, Sapporo, 1992), p. 456.
- ²⁹O. Mishima, *Nature* (London) **384**, 546 (1996).
- ³⁰K. Bennett *et al.*, *Philos. Mag. A* **76**, 413 (1997).
- ³¹L. A. Stern, W. B. Durham, and S. H. Kirby, *J. Geophys. Res.* **102**, 5313 (1997).
- ³²E. L. Gromnitskaya *et al.*, *Phys. Rev. B* **64**, 094205 (2001).
- ³³A. G. Lyapin *et al.*, *J. Exp. Theor. Phys.* **94**, 283 (2002).
- ³⁴A. D. Fortes *et al.*, *J. Appl. Crystallogr.* **38**, 612 (2005).
- ³⁵K. Echelmeyer and B. Kamb, *Geophys. Res. Lett.* **13**, 693 (1986).
- ³⁶W. B. Durham, H. C. Heard, and S. H. Kirby, *J. Geophys. Res.* **B** **88**, B377 (1983).
- ³⁷W. B. Durham, S. H. Kirby, and L. A. Stern, *J. Geophys. Res.* **102**, 16293 (1997).
- ³⁸P. R. Sammonds, *Science* **311**, 1250 (2006).
- ³⁹T. Kubo *et al.*, *Science* **311**, 1267 (2006).
- ⁴⁰T. Loerting *et al.*, *Phys. Rev. Lett.* **96**, 025702 (2006).
- ⁴¹K. Winkel *et al.*, in *Proceeding of the 11th International Conference on the Physics and Chemistry of Ice*, edited by W. F. Kuhs, (RSC, Dorchester, UK, 2007), p. 641.
- ⁴²R. J. Hemley, L. C. Chen, and H. K. Mao, *Nature* (London) **338**, 638 (1989).
- ⁴³S. Klotz *et al.*, *Nature* (London) **398**, 681 (1999).
- ⁴⁴W. Kraus and G. Nolze, *J. Appl. Crystallogr.* **29**, 301 (1996).
- ⁴⁵C. Lobban, J. L. Finney, and W. F. Kuhs, *J. Chem. Phys.* **112**, 7169 (2000).
- ⁴⁶D. C. Dunand, C. Schuh, and D. L. Goldsby, *Phys. Rev. Lett.* **86**, 668 (2001).